IMMUNOPHENOTYPING AND TWO-COLOR FLOW CYTOMETRY: STRATEGIES OF OPERATION AND LYMPHOCYTE GATING FOR SUBTYPING LYMPHOCYTE POPULATIONS IN PERIPHERAL WHOLE BLOOD OF CYNOMOLGUS MONKEYS

By

LILLI DECKER

Bachelor of Science
Dowling College
Oakdale, NY
1992

Doctor of Veterinary Medicine
Oklahoma State College
Stillwater, OK
1997

Submitted to the Faculty of the
Graduate College of the
Oklahoma State University
in partial fulfillment of
the requirements for
the Degree of
MASTER OF SCIENCE
May, 2000

IMMUNOPHENOTYPING AND TWO-COLOR FLOW CYTOMETRY: STRATEGIES OF OPERATION AND LYMPHOCYTE GATING FOR SUBTYPING LYMPHOCYTE POPULATIONS IN PERIPHERAL WHOLE BLOOD OF CYNOMOLGUS MONKEYS

Thesis Approved:

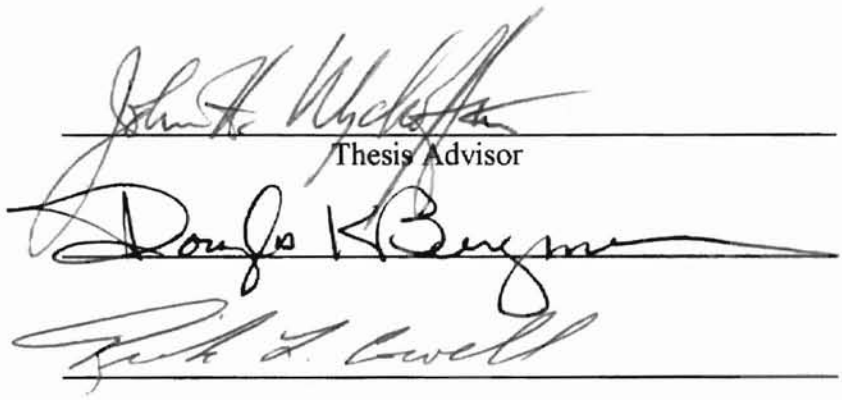

Thesis Advisor

Dean of the Graduate College

ACKNOWLEDGEMENTS

I would first like to thank Dr. Patrick Cusick of Abbott Laboratories for providing the essential instrumentation, reagents, miscellaneous supplies, and general funding for this project. His enthusiasm and encouragement was infectious, and I sincerely appreciate his inquisitive nature and keen intellect. If not for his suggestions and support, this project could not have been undertaken. I extend my sincere gratitude to my advisor, Dr. John Wyckoff, III, whose knowledge of immunology, as well as assistance, guidance, encouragement and friendship proved invaluable. I would also like to thank my other committee members, Dr. Rick Cowell and Dr. Doug Bergman for their support in the completion of this endeavor. Special thanks to Ms. Diana Moffeit, whose expertise and assistance in fulfilling the Graduate College's formal requirements for thesis format and submission were greatly appreciated. Thanks also to Mr. Mike Mahoney, Mr. Curtis Andrew, Mr. Jim Rupp, Dr. Jerry Ritchey, Dr. Jim Meinkoth, Dr. Ken Clinkenbeard and all the emergency laboratory technicians at Special Medicine for their suggestions and support during this process.

Finally, I must extend my sincere gratitude to Dr. Chris Arnold, Dr. Kathleen Sullivan, my sister Jill Decker, my brother Steve Decker, and my parents, for their assistance, encouragement, support, and understanding during some of the more frustrating moments encountered while completing this thesis.

TABLE OF CONTENTS

Chapter Page

LIST OF FIGURES

I.

INTRODUCTION

THE ANIMAL MODEL

Cynomolgus monkeys (*Macaca fascicularis*) are members of the macaque species, and represent a non-human primate that is phylogenetically similar to man. Because of this, macaques provide an excellent animal model for preclinical pharmaceutical trials, as well as the study of a variety of human diseases, most notably, acquired immunodeficiency syndrome (AIDS) and lymphomagenesis. Similarities include the organization of both their immune and hematopoietic systems, including specific cellular antigens. As a result, this similarity in cellular markers has provided an invaluable research template for a number of immunophenotyping techniques. Much of this research has been directed towards 1) identification of similar, biologically important cellular markers and cytokines among animal species 2) development and standardization of techniques that allow reproducible identification of these molecules, and 3) applications of these techniques in the study of human disease processes.

INTRODUCTION TO IMMUNOPHENOTYPING

Immunophenotyping involves the use of monoclonal antibodies (mAb), specifically designed to recognize and bind to unique, cellular antigens. Antigens may be cell-surface oriented, or located in the cytoplasm or nucleus. The mAb's are labeled with a chromophore prior to or after binding the targeted cellular antigen. Chromophores include fluorescent, enzymatic, or radioactive substances, allowing identification of targeted cell types. In this way, specific cell types may be isolated and quantified. Currently, a number of different technologic tools and methods for immunophenotyping are available, including the use of flow cytometry.

INTRODUCTION TO FLUORESCENT CYTOMETRY

Flow cytometry combines cell-sorting technology with fluorescent immunophenotyping and represents a powerful tool for the rapid identification and quantification of cells in heterogeneous populations. One clinical application of flow cytometry in human medicine is the isolation and quantification of leukocytes, specifically, lymphocytes and lymphocyte subtypes in whole blood, using combinations, or "panels" of chromophore-bound anti-human mAb's. Initial or sequential results allow quantification and identification of shifts in blood lymphocyte populations, which reflect alterations in the immune response. Current applications of this technology in human medicine include use as a prognostic indicator for patients infected with human

immunodeficiency virus (HIV), and identification and differentiation of different T- and B-cell leukemias and lymphomas.

STUDY OBJECTIVES

Duplication or reproduction of a standardized human panel in cynomolgus monkeys would provide a useful tool for preclinical efficacy and toxicologic evaluation of potential therapeutics for human diseases in an animal model. Cynomolgus monkeys are less aggressive and more manageable than other macaques. They are also cost-effective, and represent a more readily available source of animal subjects for many pharmaceutical developers. Currently, there are very few specific reagents available for the immunophenotyping of monkey leukocytes. Initial goals of this project included 1) identification of commercially available human mAb's that would cross-react with Cynomolgus leukocyte antigens, and 2) duplication or development of a standardized procedure and panel of mAb's that could be used to classify and quantify lymphocyte subpopulations using flow cytometry on Cynomolgus whole blood samples. A review of the available literature revealed several other studies with similar goals. Cross-reactivity trials of several mAb clones were necessary, and, in some instances, the primary focus in many of these studies.

Interestingly, no specific information regarding details of the actual operation of the flow cytometric technology was provided in any of this research. During this project, it became clear that the technical operation of this equipment required much experimentation and research regarding appropriate use. Because appropriately

established parameters would provide the foundation by which results were generated, detailed information regarding flow cytometric techniques used for this project are included. A comparison of these results to those of similar studies is also provided

II.

IMMUNOPHENOTYPING

CELLULAR ANTIGENS

The idea of using chemically labeled antibodies as reagents for the detection of cellular antigens dates back nearly 60 years. In the last 20 years, with the broadening of our knowledge base and the availability of improved high technologic equipment, there has been an explosion of knowledge regarding the identification of these cellular markers. This includes the elucidation not only of the presence and location of these antigens, but the structure and function as well. Central to this rapidly expanding knowledge base are cellular-signaling, and the resultant biologic response of cells to these signals.

Cellular antigens often represent cellular receptors, which, once activated by binding a specific ligand, may generate a cascade of cellular events that may have either local, or global impact on the entire organism. Normal cellular responses, as well as abnormal, have been the subject of much study. The diversity of biologic responses is extraordinary, ranging from the normal death of a single cell, to abnormal cellular proliferation resulting in cancer. Hundreds of cellular markers have been identified and studied, and many of these markers and their biologic properties, have been found to be

conserved among species. Conservation of these molecules among species allows animal resources to be used for continued research in the areas of cellular metabolism and responses. These include the elucidation of the roles of cytokines, cellular genetics, cellular activation, differentiation, proliferation and death, and regulation of the immune response.

Flow cytometry was originally developed to provide a rapid, sensitive, quantitative means of analyzing a particular cell population in a heterogeneous cell mixture. Previously, quantitative immunophenotyping was limited to traditional microscopic methods, which proved both time-consuming and subjective. The impact of the HIV/AIDS pandemic likely exerted the strongest influence on the technologic evolution of flow cytometry over the last 15 years [7]. Although experimental and clinical applications of this technology have become more diversified, research and clinical applications involving the immune response remain forefront [16]

III.

FLUORESCENT CYTOMETRY

INSTRUMENTATION AND METHODOLOGY BASICS

Flow cytometers can generate information regarding physical, biochemical, and antigenic properties of single living (or dead) cells. In general, the instrumentation requires that cell preparations be suspended in a liquid medium, or "sheath" fluid. When the prepared sample is introduced into the machine, the suspension is channeled into increasingly thinner columns, ultimately separating individual cells in a linear fashion. Individual cells are then directed past excitation laser beams, resulting in the emission of photons. Two distinct analytic measurements may be made; the angle at which the photons scatter, and their wavelength. Two parameters, designated as Forward Angle Scatter (FSC), and Side (or Orthogonal) Angle Scatter (SSC), represent the measured angle of the scattering of visible light (460 nm), and can be related to specific physical properties of the cell.

FSC distinguishes differences in cell size, while SSC represents cell complexity (mononuclear, lobularity, and granulation). The multiangle polarized scatter allows not only cell quantification, but cell sorting as well. Depending on the software used, different cell types can be graphically displayed and viewed as distinct cell populations. Figure 1 provides a graphical scatterplot representation of the distinction of blood leukocyte populations using these parameters.

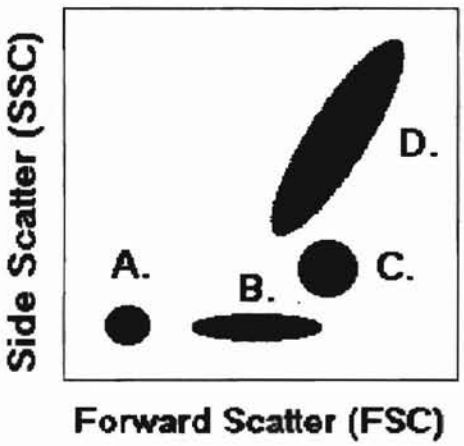

Figure 1. Graphical representation of a typical light scatter dot-plot depicting separation of distinct leukocyte populations in appropriately prepared whole blood. FSC separation is based on increasing cell size, while SSC separation is based on cell complexity. A = Cellular debris and platelets.B = Lymphocytes.C = Monocytes. D = Granulocytes.

Cellular debris and platelets are small, without much complexity, and so reflect very low FSC and SSC properties. Lymphocytes are small, mononuclear cells, reflected by low FSC and SSC properties. Granulocytes are larger cells, reflected by increased FSC. Segmented nuclei and presence of granules translates into a very high SSC signal. Monocytes are large cells, emitting a high FSC signal, with intermediate nuclear and cytoplasmic complexity, resulting in an intermediate SSC signal.

FLUORESCENT SCATTERING

Flow cytometers also employ additional excitation sources that operate at a single- or narrow-band wavelength, restricting photon emissions to those of a similar wavelength. These lasers are designed to generate photons from fluorescent chromophores, which may be conjugated to mAb's (fluorescent probes), and can be bound to cells. (i.e., "stained" cells). A few examples of commonly used fluorescent probes include mAb-bound peridinin chlorophyll A protein (PerCP), fluorescein isothyocyanate (FITC), and R-phycoerythrin (PE), which emit photons of wavelengths of 670 nm, 530 nm, and 575 nm, respectively. These probes can be used alone, or in combination to analyze unique antigenic determinants on or within individual cells, delineating different cell populations.

Because the fluorescent wavelengths relate to colors of the spectrum, different chromophores are often referred to in terms of a specific color (FITC = green, PE= red, etc.) When more than one probe is utilized on a single cell preparation (i.e., two-, three- and four-color flow), the chromophores are segregated as numerical parameters, such as Fluorescent 1 (FL1), Fluorescent 2 (FL2), etc. Figure 2 depicts an example of the graphical representation of data generated on a fluorescent plot using two-color fluorescence.

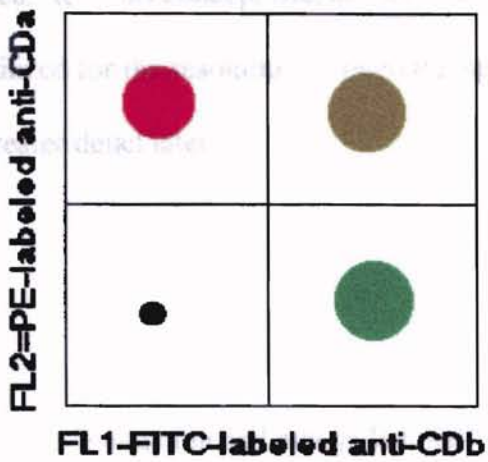

Figure 2. Graphical representation of typical two-color fluorescent labeling depicting separation of cell populations based on antigenic properties. Two unique antigens are described as CDa and CDb. These are targeted by chromophore labeled monoclonal antibodies (mAbs) specific for each antigen as indicated. As intensity of FITC or PE fluorescence increases, clouds move farther along the x or y-axis, respectively. Upper left quadrant: Cells expressing CDa only. Lower left quadrant: No expression of either antigen (unstained or negative cell population). Lower right quadrant: Cells expressing CDb only. Upper right quadrant: Cells expressing both antigens CDa and CDb.

Currently, a vast array of unconjugated chromophores, unconjugated species-specific mAb's, as well as conjugated probes, are commercially available. Which probes are chosen depends on the animal species used for the study, known cellular antigens of the cell population of interest, and the experiment or protocol design. Flow cytometric immunophenotyping involves two important parameters, which can be distinctly measured: the wavelength emitted, and the intensity of the emission. If antigens are unique to a cell type, these cells, when stained, are easily identified by the wavelength of the photons emitted. However, because some antigens are shared among different cell types, evaluation of wavelength alone would be unreliable as a means of identification when a heterogeneous sample, containing cell types that cross-react with certain mAb's, is evaluated.

Fluorescent intensity is directly related to the concentration of cellular antigen expressed. Because of this, if the level of antigenic expression is known among the cell types under investigation, the degree of intensity can be used to resolve cross-reacting cell populations. In this way, cell types may be sorted not only on the basis of the fluorescent wavelength emitted by cells bound to probes, but by their staining intensity as

well. It is this concept that allows a commonly used reagent pair (CD45/CD14) to be utilized for the resolution of overlapping cell populations, which will be discussed in greater detail later.

GATING CONCEPTS

Evaluation and manipulation of the data generated by the above-mentioned parameters is performed using cytometric software. Cytometric software varies from instrument to instrument, but all software can display data in numerical, as well as graphical form. Software is typically designed for specific applications, with a number of different protocols for their utilization.

For this project, the Becton-Dickinson FACSCalibur Instrument, and CELLQuest software was used. This software is well suited for the sorting and evaluation of the heterogeneous leukocyte populations found in whole blood. With CELLQuest, individual cells, or "events" can be visualized using histograms, contour plots, and scattergrams. Because scattergrams have traditionally been used in the evaluation of peripheral blood leukocytes, this graphical representation was chosen for this project. The scattergrams, or "dot-plots" include an x- and y-axis, which can be defined by the operator as a function of the measurable parameters of light-scatter (FSC, SSC), and fluorescent scatter (FL1, FL2, etc.), in either linear or logorhythmic scale. All events displayed can be analyzed and numerically quantified based on the parameters chosen. Further, graphical events can be isolated, by confining them to a "region" (R1), or quadrants, which can be defined (or drawn) directly on the graph by the operator. Similarly, all events in regions

or quadrants can be numerically quantified. A second graph may then be constructed, this time using different parameters, and formatted to display only the events that were contained within R1, a procedure known as "gating". The operator may define the gate corresponding to R1 in any way. For simplicity, gates are often defined using the same enumeration as the region it is related to. Thus, the gate corresponding to R1 may be defined as G1. Multiple regions may be drawn, and multiple gates chosen for display on a single graph. In this way, events isolated by light scatter properties, may be viewed through a gate that was defined using fluorescent scatter, and vice versa. This procedure is known as fluorescent gating, or "backgating". Gating allows the visualization of only events that meet the criteria of all operator-chosen parameters. This sequential process allows the operator to isolate, purify, and enumerate a targeted cell population, based on the successive confinement of events by the parameters chosen for each graph.

OPTIMIZATION TECHNIQUES

Operation of flow cytometers requires a certain skill level involving the instrument controls, software, and known parameter properties of specific cell populations. Calibration techniques are varied, specific for the instrument used, and generally straightforward. Instrument optimization techniques, however, are more complex, and require some knowledge of the signal processing incorporated by flow cytometers. Photomultiplier tubes (PMTs) and photodiodes are two types of photon detectors utilized by flow cytometers. Photodiodes are less sensitive to light, and are used to detect only strong light signals, such as FSC. Signals emitted for any of the

measurable parameters may be individually diminished or increased by adjusting specific amplifier gain controls. PMTs are used to detect the weaker signals emitted by SSC, and FL. In addition to amp gain, the voltage of PMTs may also be adjusted, or "multiplied", resulting in changes in signal strength. Thus, voltage adjustment result in large changes in signal strength, while adjustments of amperage gain allows "fine-tuning", or "tweaking" of the signal.

When evaluating samples using flow cytometry, it is important to include as much of the cell population of interest as is possible. This requires that the operator be able to recognize and distinguish events that represent known cell population distributions, from events that are secondary to debris (cell fragments) and platelets. FSC and SSC may be adjusted to minimize debris, and maximize cell populations of interest. An example of how cell populations may be adjusted using these parameters is provided in Figure 3. A limiting threshold level may also be set to exclude undesired noncellular events along the FSC axis as indicated.

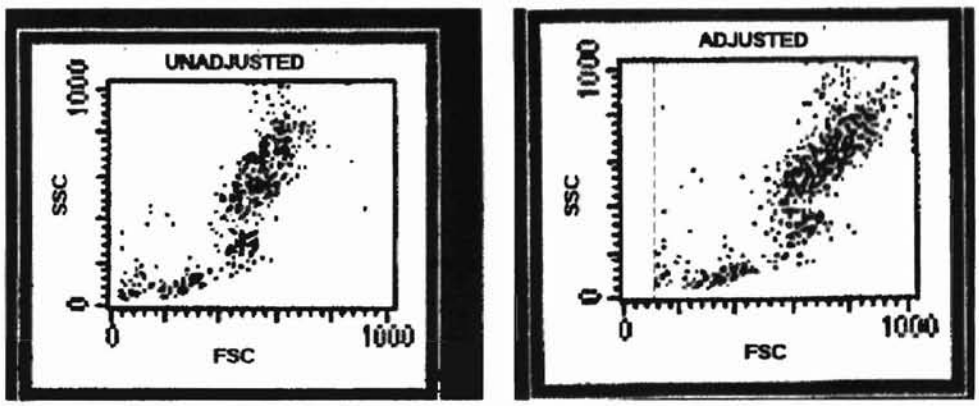

Figure 3. Optimization of FSC and SSC amperage gain and SSC voltage controls allows distinction of cell populations and detection of most cellular events. Additional adjustment of FSC limiting threshold allows exclusion of noncellular events, and is represented by the dotted line on the second dot plot above. All events to the left of this line are excluded.

Other instrument adjustments are concerned with fluorescent optimization. Adjustments are necessary to minimize interfering fluorescence secondary to non-specific mAb binding, and autofluorescence. Isotypes of immunoglobulin G (IgG) are most commonly used to manufacture mAbs. Individual immunoglobulin molecules contain two potentially reactive moieties, the Fc and FAb regions. It is the FAb region of mAbs that is engineered to recognize, and bind to, specific epitopes of interest. However, many cell types express receptors that non-specifically bind the Fc region of IgG antibodies. In addition, some non-stained (or "negative") cells may emit varying intensities of inherent autofluorescence. These non-specific sources of fluorescence, termed "background fluorescence" can, and often do, interfere with measurements of fluorescence emitted by stained cell populations of interest. Therefore, the use of properly designed negative controls is critical.

Negative controls should be engineered from the same antibodies as the probes, but without FAb specificity for the antigens being analyzed. Using antibody isotypes similar to the probes, but specific for a different species often attains this goal. They should be labeled with the same fluorescent chromophores as will be used on the sample under investigation. Thus, when negative controls are added to a sample of unstained cells (i.e., not bound to specific probes), only background fluorescence will be emitted. Both fluorescence and autofluorescence, emitted respectively by non-specific binding of negative controls and non-staining cells in the sample, can be reduced by adjusting the voltage and amperage of the photomultiplier detector (s) for each fluorescent wavelength (optimization of fluorescence). For two-color flow cytometry, using CELLQuest

software, this is performed by shifting the events that represent background fluorescence into an operator-defined LL quadrant on a FL1/FL2 scattergram (Figure 4).

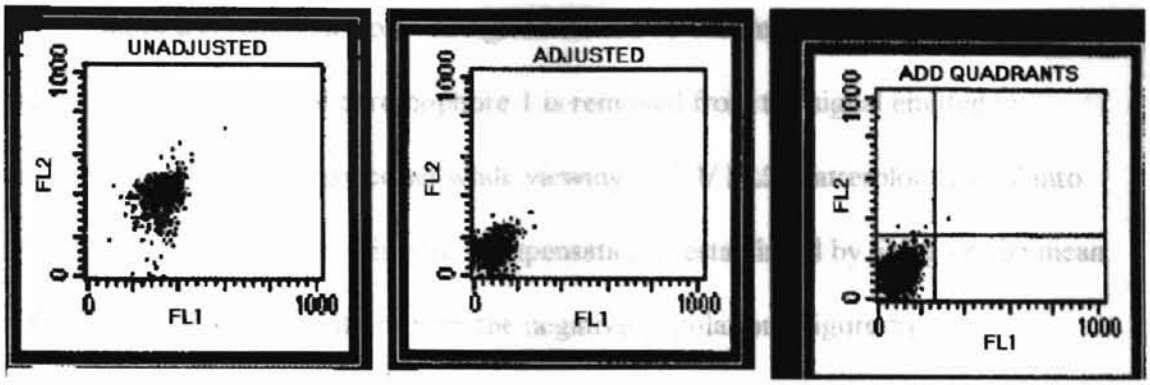

Figure 4.Optimization of fluorescence. Either an unstained cell sample and/or an IgG isotype control may be used to minimize autofluorescence and non-specific fluorescence (together termed "background" fluorescence), respectively. These nonspecific events are shifted to the lower left quadrant on a fluorescent plot by adjusting FL1 and FL2 amperage and voltage.

When using multiple chromophores in a single sample preparation, the most important adjustment involves optimization of fluorescent compensation. Often, fluorescent emissions from different chromophores may overlap spectrally. This is especially evident when a single excitation beam is used to excite different chromophores. Expanding the number of excitation lasers allows a better physical and kinetic separation between signals, but many of the cytometers currently available are not this well-equipped due to the expense of additional lasers.

Fortunately, current technology provides a means to compensate for this spectral overlap. Electronic compensation requires single stained samples, each containing a single fluorescent probe. Alternatively, a single sample, combining all probes to be utilized, can be used, provided that it contains cells that uniquely bind only one type of probe. When multiple probes are used in a single sample, compensation voltages are adjusted by subtracting the signal of chromophore A that is measured as a function of

chromophore B, from the signal emitted by chromophore B, and vice versa. CELLQuest software provides specific voltage controls, termed FL1-%FL2 (where spectral overlap of chromophore 2 is removed from the signal emitted by chromophore 1), and FL2-% FL1 (where spectral overlap of chromophore 1 is removed from the signal emitted by chromophore 2), which may be set while viewing a FL1/ FL2 scatterplot divided into user-defined quadrants. In this way, compensation is established by lining up the mean of the FL1 and FL2 populations with the negative population (Figure 5).

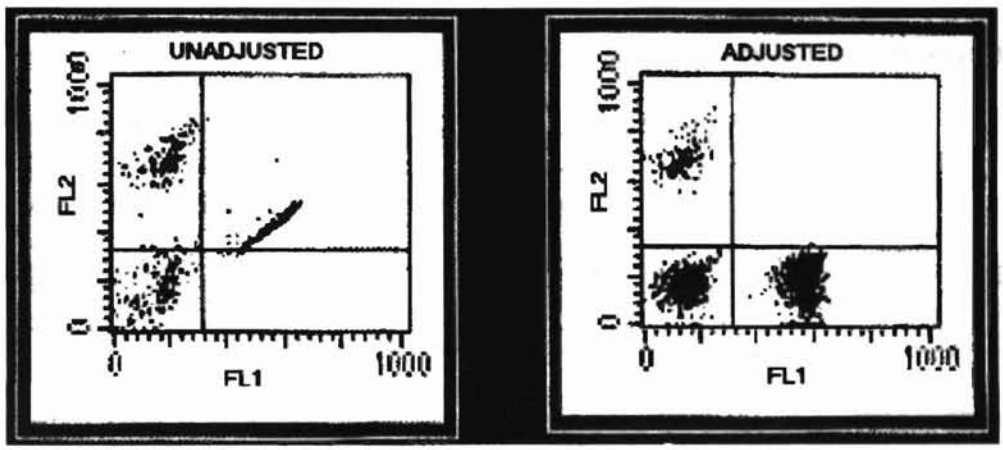

Figure 5. Optimization of fluorescent compensation. Compensation voltages are adjusted to reduce spectral overlap between chromophores. The mean of FL1 and FL2 are shifted to line up with the mean of the nonspecific events ("unstained" events).

Although more involved, a similar process is used for compensation optimization when using three- or four-color flow. Again, procedures regarding all optimization techniques will be specific for the cytometer being utilized and are provided by the manufacturer.

LYMPHOCYTE SUBTYING

Terminology of cellular antigens is, at best, confusing. This may be a reflection of the rapidity at which the same antigens have been discovered and named by different researchers. As a result, several notations may reference one cellular antigen. Recent attempts to establish a universal reference system have resulted in the "CD" numbering system.

Specific antigens are labeled as numerical CD or "clusters of differentiation"; this notation will be used here. A number of unique lymphoid cell-surface markers have been identified, and are commonly utilized to target and quantify specific lymphocytes in flow immunophenotyping. These include CD3, specific for all T lymphocytes (except Natural Killer cells), CD20, specific for B-lymphocytes, and CD56 and CD16, specific for Natural Killer (NK) cells. T-cell subtypes can further be classified as T-helper lymphocytes (Th) which express CD3, and CD4, but are CD8 negative (CD3+, CD4+, CD8-), and cytotoxic T-lymphocytes (CTL), which express CD3 and CD8, but are CD4 negative (CD3+, CD8+, CD4-).

The availability of mAbs that specifically bind these unique antigens has allowed lymphocyte sub-typing and quantification using flow cytometry. Proper flow cytometric analysis of lymphoid cells in whole blood requires that the lymphoid population be isolated from other cell types, which can be established by defining a "lymphocyte gate". The National Committee for Clinical Laboratory Standards (NCCLS) has described certain guidelines regarding quality assurance for flow cytometric lymphocyte immunophenotyping, which include minimal requirements for gate "purity" and

"recovery" when establishing optimal lymphocyte gates. Gate purity refers to the percentage of lymphocytes within the defined lymphocyte light-scattergate (FSC/ SSC), relative to all other non-lymphoid events within the same gate. Recovery refers to the percentage of lymphocytes within the light-scattergate relative to the total number of lymphoid events recorded in the original sample acquisition. Depending of the reference, purity and recovery are recommended to optimized to at least $> 80\%$, and $> 90\%$, respectively [3,5,8,16].

One commonly used protocol for performing lymphocyte analysis on peripheral whole blood includes the use of a CD45/CD14 reagent pair. The protocol allows the establishment of an optimal lymphocyte gate by adjusting gate characteristics of purity and recovery as a quality control measure.

ESTABLISHING THE LYMPHOCYTE GATE USING CD45 AND CD14 ANTIGENS

For two-color flow immunophenotyping of peripheral blood lymphocyte analysis, it is necessary to aliquot the specimen into several sample tubes, each containing combinations of two-color mAb reagents; the paired reagents are collectively referred to as a "panel". Most commonly used panels consists of six two-color reagent pairs, exploiting the specific lymphocyte antigens previously mentioned, as well as two additional antigens, CD45 and CD14, and a negative control. Figure 6 shows the typical probe pairs used.

Tube1:	Negative isotype controls FITC-IgG / PE-IgG
Tube 2:	Unstained sample
Tube 3:	FITC-CD45 / PE CD14
Tube 4:	FITC-CD43 / PE CD4
Tube 5:	FITC-CD3 / PE CD8
Tube 5:	FITC-CD3 / PE CD20
Tube 7:	FITC-CD3 / PE CD16 and PE-CD56

Figure 6. Typical monoclonal antibody probe pairs used for lymphocyte immunophenotyping.

The IgG FITC/IgG PE paired sample is used for optimization procedures, and to define the negative population, as previously described. The CD45 FITC/CD14 PE reagent pair is used to establish the optimal lymphocyte gate while maintaining quality control. CD45 is a pan-leukocyte cell-surface antigen that is present on granulocytes, monocytes, and lymphocytes. However, each cell type expresses it in different concentrations. Because of this, probes using CD45 mAbs may be used to distinguish leukocyte populations based on their different staining intensities.

Cells exhibiting increasing numbers of cell surface CD45 antigens will stain with increasing fluorescent intensities. Granulocytes stain the weakest (dim), lymphocytes stain the brightest (bright), and monocytes exhibit intermediate staining intensity. This single parameter is insufficient to distinguish these cell populations, however, because significant overlap exists in the intensity distributions. This overlap may be resolved with the use of CD14. CD14 is expressed in high levels on monocytes, and dimly on mature neutrophils. By combining CD45 and CD14, it is possible to differentiate these cell populations based on their immunofluorescence, using two different chromophores, while viewed on a FL1/FL2 scattergram using this reagent combination allows the operator to define a lymphocyte gate, via backgating.

This backgating process is depicted in a step-wise fashion in Figures 7a-f. A sample stained with CD45 FITC/CD14 PE is first displayed on an ungated FL1/FL2 dot plot. FL1 is typically defined on the x-axis, representing increasing intensity of FITC staining by cells. FL2 is defined on the y-axis, representing increasing intensity of PE staining of cells. Although all leukocytes stain with CD45 FITC, the monocytes will also be stained with CD14 PE (CD45+ and CD14+), allowing visualization of three distinct cell populations, and an area that represents the negative population. Regions are then defined by the operator, segregating these populations (Figure 7a). The region (R1) that is defined for the lymphocyte population (bright CD45+, CD14-) must be large enough to include all the lymphocytes in the sample, i.e., the total number of lymphocytes. Defining a large region, however, reduces the purity of the lymphocyte population by including CD45+/CD14- monocytes, and possibly some CD45+ granulocytes. A smaller region, although representative of a more pure lymphocyte population, is likely to exclude some lymphoid events, reducing lymphocyte recovery. It is clear that there exists an indirect relationship between purity and recovery. The events in R1 are then displayed on a light-scatter (FSC/SSC) plot, which is gated on R1. A new region (R5) is drawn to include only the cells with low SSC, which

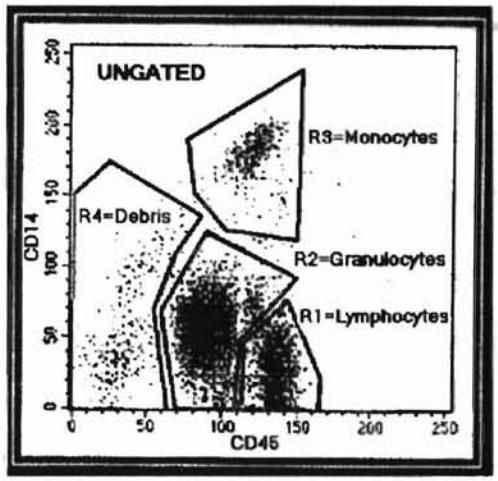

Figure 7a. Defining regions that isolate different leukocyte populations based on antigenic properties of light scatter using CD45 and CD14

represent lymphocytes (Figure 7b). The exclusion of the high SSC cells, which represent monocyte and granulocyte contamination within R1, further purifies the lymphocyte population. It is, in fact these CD45 bright and low FSC properties that define the lymphocyte population. The light-scatter plot is then reformatted to remove the R1 gate. All events measured in the sample are now displayed (Figure 7c). The events within R5 are then backgated to the original regions drawn on the FL1/FL2 scatter plot, this time gated on R5 (Figure 7d). The events that now fall within the R1 region should represent a

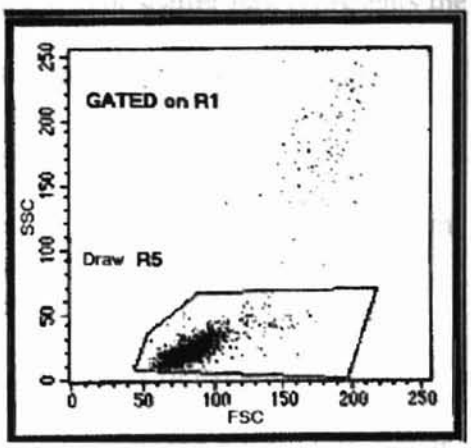

Figure 7b. Define R5 on light scatter plot adjusted to display only events contained within R1

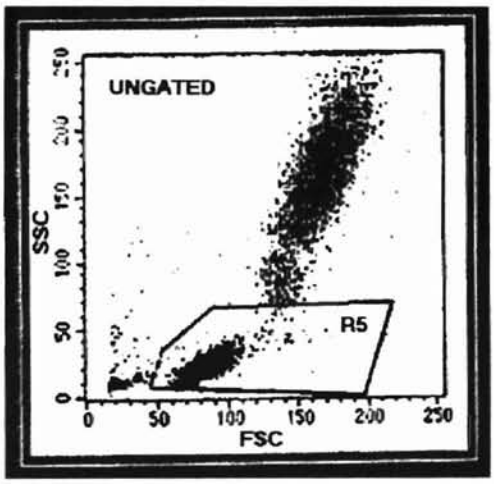

Figure 7c. Remove gate to display all events of fluorescent dot plot in light scatter gate.

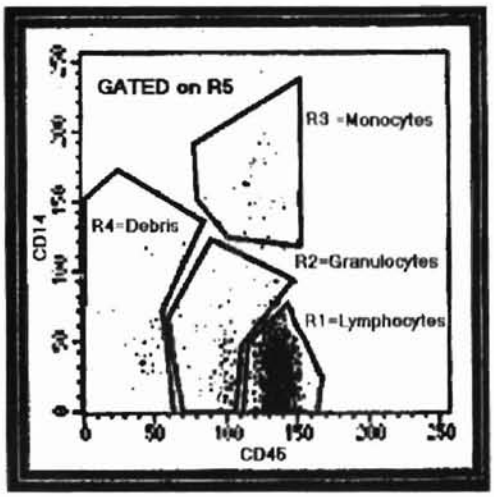

Figure 7d Backgated to display only events of R5 region on fluorescent dot plot.

pure lymphocyte population. The R5 region drawn on the light scatter plot represents the lymphocyte gate, and can be optimized to fulfill NCCLS guidelines of recovery and purity.

Percent (%) Lymphocyte Recovery is defined as the number (#)of lymphocytes in the light scattergate, divided by the total number of lymphocytes in the sample, and multiplied by 100. This may be calculated by dividing the number of events backgated from R5 (light-scatter, ungated) and displayed in the R1 region of the fluorescent scatter plot (gated on R5), by the number of events confined to the R5 region drawn on the light-scatter gate (gated on R1).

Percent (%) Lymphocyte Purity is defined as the number (#) of lymphocytes in the light scattergate, divided by the # of events in the light scattergate, and multiplied by 100. This may be calculated by dividing the number of events backgated from R5 (light-scatter, ungated) and displayed in the R1 region of the fluorescent scatter plot (gated on R5), by the number of events in the R5 region of the light-scatter gate (ungated).

Optimization of the lymphocyte gate is performed by defining a new region (R6) on the same light-scatter plot, and reformatting the graphs appropriately, so that R6 data replaces R5 data (Figure 7e). Using the above calculations on the data collected, R6 is adjusted until the criteria for recovery and purity is attained, establishing the lymphocyte gate. Data is then collected from the events backgated to the

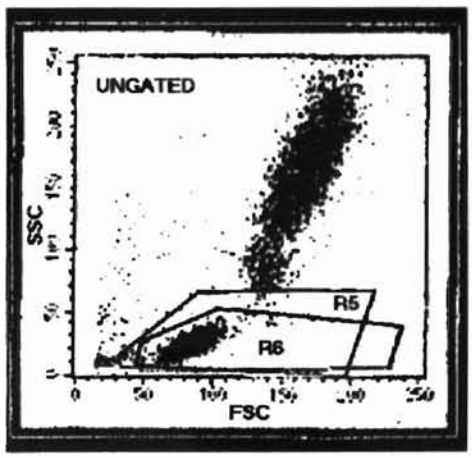

Figure 7e. Create and adjust R6 for optimization of purity and recovery.

fluorescent scatter plot , which is formatted to display only events contained within the final R6 region of the light scatter plot. (Figure 7f). All remaining paired samples are evaluated using this established gate and all data collected and instrument settings may be saved in a data file for later evaluation or use, respectively.

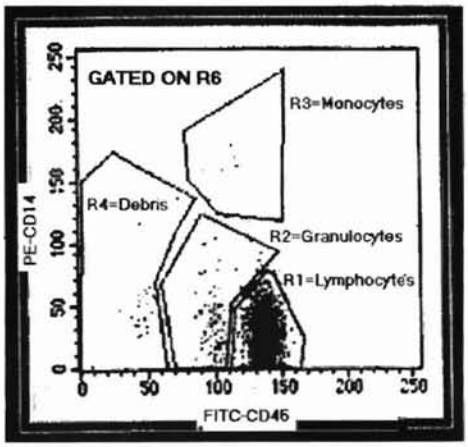

Figure 7f. Calculations for purity and recovery utilize data collected from fluorescent scatterplot gated to display only events contained within the R6 region.

IV.

REVIEW OF THE LITERATURE

Early attempts at subtyping cynomolgus, as well as other non-human primate lymphocytes, included delineation of basic B and T subtypes using techniques established in humans with anti-human monocolonal antibody reagents. These included spontaneous rosetting of T lymphocytes with sheep erythrocytes (where the erythrocyte receptor was antigenic determinant T11, a CD2 epitope), and alpha-naphthyl-acetate esterase (ANAE) staining [11,12] Separation of cell lines using these techniques was subjective, as distinction of T and B subtypes was based on staining intensities assessed via light microscopy. Because no specific anti-monkey MAbs were available, much research regarding lymphocyte subsetting in cynomolgus monkeys has included cross-reactivity trials.

The earliest attempts to delineate cynomolgus peripheral blood lymphocytes using flow cytometry focused primarily on cross-reactivity trials with available anti-human MAbs [6]. One color flow was used to evaluate several FITC labeled anti-human CD2 (T11, T12), CD4 (T4, T4a) and CD8 (T8, T5, T8b, T8c) clones. 37 non-human primates, including 7 adult cynomolgus monkeys were utilized, and results were pooled. Blood leukocyte isolation was performed using the Ficoll-Hypaque density gradient. The method for delineating cell populations is described as "cytofluorographic analysis of cell

populations was performed on a fluorescent-activated cell sorter" (FACS-I, Becton-Dickinson, Mountainview, CA). This early attempt did not utilize any specific lymphocyte gating technique, and data was expressed as the percent of positively staining cells. Cross reactivity was noted in several of the mAb clones used, resulting in the conclusion that these findings "support the notion that the degree of sharing of T-cell specific surface antigens between man and other primate species reflects the phylogenetic distance between them. Moreover, they raise provocative issues concerning the potential uses of mAbs in elucidating both structural and functional roles of these T cell-specific structures"

In 1990, Sagara, et al, compared the rapidity and precision of the ANAE technique to that of one-color flow cytometry [10]. An anti-human T11 mAb (CD2 antigenic determinant) was used as a pan-T cell marker, and goat-anti-monkey IgG was used to target B cells; FITC was used to label all antibodies. Isolation of blood leukocytes was performed using a Percoll density gradient, and lymphocyte subtyping was based on enumeration of mononuclear cells that reacted with each antibody. One again, a specific lymphocyte gating technique is not described. In this study, the correlation coefficient (r) revealed flow cytometry to be more precise, as well as advantageously more rapid than the ANAE immunophenotyping technique.

In 1993, Bleavins, et al, used one color flow to assess cynomolgus peripheral blood lymphocyte populations in whole blood, using a lysing agent (ammonium chloride), rather than a density gradient technique [2]. PE labeled anti-human clones for CD4 (anti-leu 3a), CD8 (anti-leu 2a, and CD20 (anti-leu 16) were assessed. Values derived from 146 cynomolgus blood samples were compared to known human ranges, and it was

determined that the CD4/CD8 ratio was reversed from that of humans. Further, preparation from peripheral whole blood using a lysing agent, rather than a density gradient technique, was advocated as it allowed concurrent evaluation of hematologic and clinical biochemistries using only a single, small sample. This article does mention a gating technique wherein "lymphocytes were gated from other leukocyte types based on forward and 90 degree light scatter". Lymphocyte subpopulation values as well as hematologic values were provided in this paper.

In 1995, Verdier et al used two-color (PE and FITC) flow cytometric immunotyping to investigate cross-reactivity of commercially available human reagents with cynomolgus monkey lymphocytes [14]. A number of anti-human mAb clones including CD2, CD4, CD8, and CD20 were evaluated. In this expanded study from earlier research [32], lymphocyte subtype values on lysed whole blood of 312 adult cynomolgus monkeys were obtained. Speculation of discrepancies as well as similarities in these results compared to other research focused on a possible differences in binding affinities of the mAb clones used among the studies. Because of the large number of subjects, and the wide variety of clones tested, a panel of specific MAbs was proposed for cynomolgus subtyping. Again, as with the Bleavins research, a comparison of these results to established human ranges revealed a reversed CD4/CD8 ratio. One again, the gating technique is characterized as "the gate was defined to include cells showing human lymphocyte parameters for forward and right-angle light scatter; the gate was regularly checked with both human and monkey samples. A total of 3000 lymphocytes was recorded for each sample". Further, that "cells with a high fluorescent intensity were compared with unstained cells in the same sample and with cells from the control blood

sample and were identified as positive cells for the lymphocyte subset under study. MAbs were classified in two groups, namely those which provide clearly identified stained cell sub-populations comparable to human cells and those which did not allow differentiation of two populations of stained and unstained cells. Data were assessed qualitatively but no statistical analysis was performed". This suggests that the lymphocyte gate was established based on low scatter properties only, without gate optimization.

Two later studies focused on comparisons between cynomolgus adult and neonatal values of CD4 and CD8 lymphocytes. Both of these studies used whole blood sample preparations and two-color flow immunophenotyping. Although Baroncelli, et al, focused on neonatal parameters, results for 37 adult cynomolgus monkeys were provided [1]. In this research, "10,000 lymphocytes, gated from leukocyte types based on forward and 90 degree light scatter, were analyzed for each sample by using a FACScan cytometer (Becton-Dickinson). This research reported no significant sex differences, however, the reversed CD4/CD8 ratio from that of humans was once again observed. Tryphonas, et al evaluated CD4 and CD8, and included CD16 and CD20 values for 12 cynomolgus infants [13]. Much more detailed information regarding the actual operation of the FACScan flow cytometer utilized for this research was provided than in any previous study. This included basic instrument calibration using CaliBRITE beads as a reference standard. An AutoComp program was utilized to perform three FACScan adjustments, including singular event gating, PMT gain, and fluorescent compensation. Finally, a QuickCal kit, was utilized on a daily basis, allowing channel targeting and subsequent comparisons of fluorescent intensity measurements. Leukocyte separation was performed using the Ficoll-Hypaque density gradient, and lymphocyte subtyping was established on the basis

The basis of fluorescent intensity. Although "results were compiled as percentage of the lymphocyte gate and as absolute counts (x 10^6 cells/ml) using the leukocyte count", no specific information regarding establishment or optimization of a lymphocyte gate is provided. Interestingly, this research revealed a population of CD8+ CD2- lymphoid cells not previously reported to be present in adult humans or adult cynomolgus monkeys [10]. Appendix B summarizes these studies, as well as the reported lymphocyte subset values. Averaged results for this project are included.

V.

MATERIALS AND METHODS

OVERVIEW

Following cross-reactivity trials, a panel of reagent pairs duplicating those listed in Figure 6 would be used to establish an optimal lymphocyte acquisition gate. Once established, samples from nine healthy cynomolgus monkeys would be analyzed to evaluate the distribution of peripheral blood lymphocyte subpopulations. Population classifications included T-helper cells, cytotoxic T cells, B cells, and NK cells.

ANIMALS

Nine normal adult Cynomolgus monkeys (*Macaca fascicularis*) housed at Abbott Laboratories Experimental Animal Facility (Abbott Park, IL), were available for use in this study. Animals were utilized in accordance with Abbott IACUC animal use protocols. Whole blood was collected via venipuncture of the femoral vein while non-anesthetized animals were restrained in plexiglass restraint chairs. Restraint time was limited to the time necessary to collect the samples.

MONOCLONAL ANTIBODIES

A total of twenty-six mAbs, defining ten clusters of differentiation (CD markers), most of which were specific for human leukocytes, were tested to determine cross-reactivity with cynomolgus leukocytes. These antibodies are listed in Appendix A. Clones were obtained from Becton-Dickinson Immunocytometry Systems, San Jose, CA; Dako Inc; Carpenteria, CA; Biosource International, Camarillo, CA; Coulter Immunotech, France; Pharmingen Inc., San Diego, CA; and Serotec Ltd., Oxford, England. All mAbs used were purchased as pre-conjugated probes. The amount of mAb used was that suggested by the manufacturer, either neat, or at recommended dilutions. Additional dilutions were also prepared and analyzed.

CELL PREPARATION

Unrefrigerated whole blood samples were prepared within 6 hours of collection. Direct immunofluorescent staining was performed by combining 100 ul of EDTA anti-coagulated blood, with the recommended concentrations and dilutions of mAbs, in 12 x 75 mm Falcon tubes. This mixture was incubated on ice in the dark for 30 minutes. Red cells were then lysed using a commercial lysing agent (FACS Lysing Solution, Becton-Dickinson) in accordance with the manufacturer's guidelines. 2 ml of (1X) FACS Lysing Solution was added to each tube, vortexed at low speeds for 3 seconds, and then incubated for 10-12 minutes at room temperature, in the dark. Samples were then centrifuged (1500g/2800 rpm) for 3 minutes at 4 C, and washed twice with 2 ml of cold

PBS. Cells were suspended with 150 ul of PBS/0.5 % formaldehyde. Stained cell preparations were stored at 4 C, and analyzed within 48 hours. Prior to analysis, samples were diluted with 750 ul of cold PBS. Preparations were then vortexed and analyzed directly from the Falcon tubes. Tubes containing unstained cells, and FITC- and PE-labeled isotype controls were also prepared for each sample.

FLOW CYTOMETRIC ANALYSIS

Samples were analyzed on a FACSCalibur Flow Cytometer EO997 (Becton-Dickinson) using a 15 mW 488 argon-ion laser to excite FITC or PE probes. Initial instrument calibration was performed with CaliBRITE standard fluorescent beads (Becton-Dickinson) using FACSComp version 4.0 software. CELLQuest software was used for the acquisition of experimental data. Unstained cell samples, and fluorescent-labeled isotype controls were used optimize fluorescence signals, compensation, and setting of quadrant markers as previously described. Quadrant markers were set to exclude less than 2 % of the acquired events. Ungated light- and fluorescent scattergrams were used to identify cross-reactivity of probes. A number of trial runs were performed, using both human (as a control) and cynomolgus sample preparations. A series of dilutional trials were also performed. Following cross-reactivity studies, a minimum of 10,000 events within the established lymphocyte gate was acquired for analysis

COMPLETE BLOOD COUNTS

Automated cell counts and leukocyte differentials were performed on each EDTA-anticoagulated cynomolgus blood sample using the Abbott CellDyne Hematology Cell Counter series 3500 (Abbott Laboratories, Abbott Park, IL). Cell size discriminators were set on parameters optimized for non-human primates. Only samples that contained at least 3.5×10^3 WBC/ul were used.

VI.

RESULTS

PRELIMINARY FINDINGS

More detailed information regarding the monoclonal antibody clones tested for the cross-reactivity trials is listed in Appendix A, as previously stated. Anti-monkey CD3 clones were commercially available, and all clones tested exhibited strong cross-reactivity. All anti-human CD4, CD8, and CD20 clones tested were positive. Only one of the CD14 clones tested cross-reacted (Pharmingen M5E2), and only very dim-staining was noted by one of the CD56 clones (Becton Dickinson MY31). No cross-reactivity was observed with any of the CD45 or CD16 clones evaluated.

Whenever possible, clones were chosen based on previously reported positive cross-reactivities with cynomolgus or other macaque blood lymphocytes. None of the CD16 clones tested for this project showed any reactivity. Non-reactivity of CD16 clones B-E16 (Biosource) and 3G8 (Coulter) represents a discrepancy with findings of Sopper, et al, where cross-reactivity of these clones was positive. Rhesus monkeys, rather than cynomolgus monkeys were used, however, which suggests distinction in similar targeted cellular antigens between these two macaque species.

ALTERNATIVE GATING

The original goal of creating a lymphocyte panel, which included establishment of an optimal lymphocyte gate utilizing the CD45/CD14 reagent pair technique, could not be accomplished, primarily due to non cross-reactivity of the CD45 clones tested. Funding limitations precluded additional testing of other available CD45 clones. An alternative gating strategy maintaining NCCLS standards was designed for this project.

Instead of the CD45/CD14 reagent pair, this protocol proposed and utilized a triple-antibody cocktail, containing FITC-labeled CD3 and CD56 in combination with PE-labeled CD20 to establish and optimize the lymphocyte gate. The rest of the panel, including fluorescent labels, remained essentially unchanged from that listed in Figure 6. Because no cross-reacting CD16 was found, only CD3 and CD56 were combined tube 7. FITC-IgG1 and PE-IgG1 isotype controls were used. Actual clones selected and utilized are listed in Appendix B. The same backgating protocol as used for the CD45/CD14 gate optimization was followed, and a stepwise graphical illustration of the following gating technique is provided in figures 8a – 8h.

Following standard instrument calibration and optimization, and appropriate unstained and IgG isotype control configuration as previously described, a prepared sample containing the triple-reagent probe combination was introduced into the flow cytometer. Figures 8a and 8b depict the resultant FL1/FL2 and light (FSC/SSC) scatterplot, respectively.

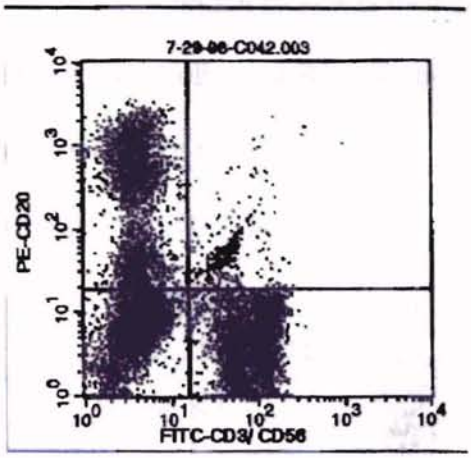

Figure 8a. Fluorescent dot-plot of FITC CD3/CD56 and PE-CD20 (ungated)

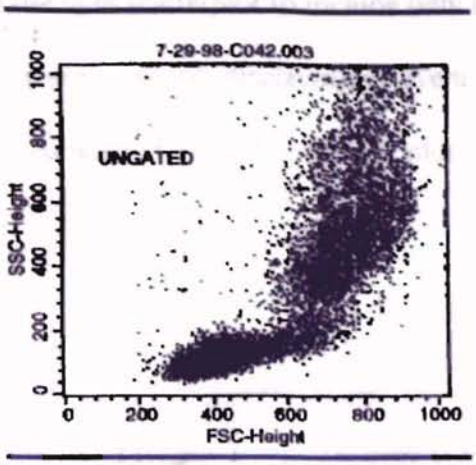

Figure 8b. Ungated FSC and SSC of CD3/CD56 and CD20

Two regions were then defined. R1 was defined to include PE-CD20 events, and R2 was defined to include the combined FITC-CD3/CD56 events (Figure 8c). These events were then displayed on the light scatterplot, which was formatted to include only R1 and R2 events through gates 1 and 2 (G1 and G2) (Figure 8d).

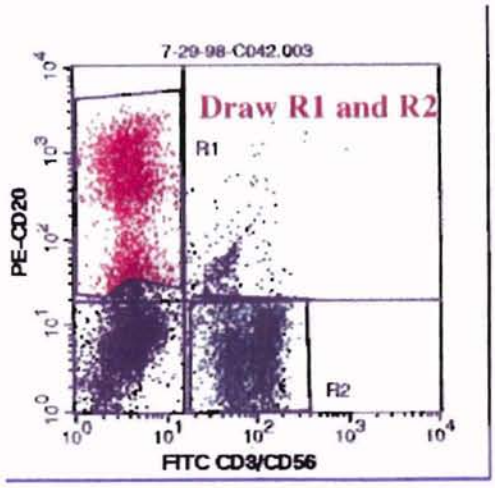

Figure 8c. Define regions R1 and R2 on fluorescent plot which correspond to B lymphocyte population and T and NK lymphocyte populations, respectively

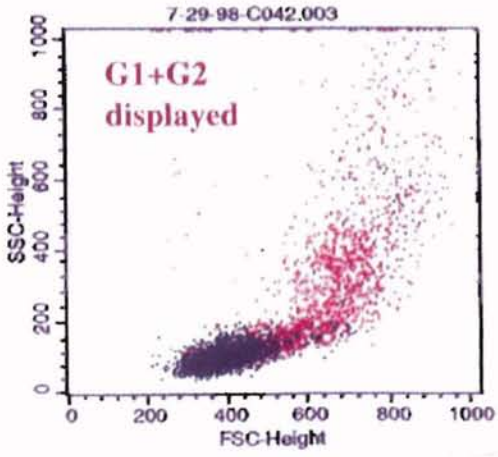

Figure 8d. Display R1 and R2 on light scatter plot which is gated to display only these selected regions (G1 and G2).

A new region (R3) was then defined on the light scatterplot to include only low SSC events. Following R3 definition, the gates were removed, displaying all events in the sample (Figure 8e). The events in R3 were then backgated to the fluorescent plot, which was gated on G3 (Figure 8f).

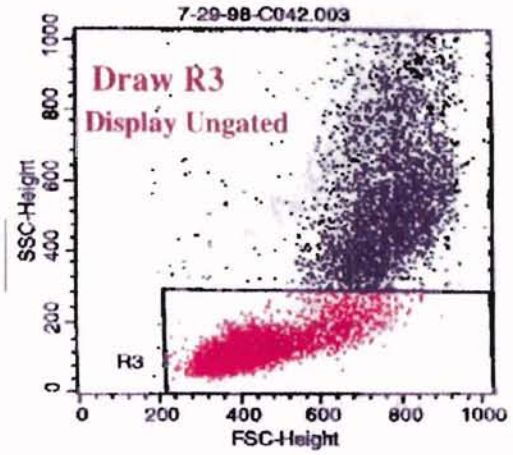

Figure 8e. A region defined as R3 is created on R3 are backgated to the fluorescent plot, and displayed as G3

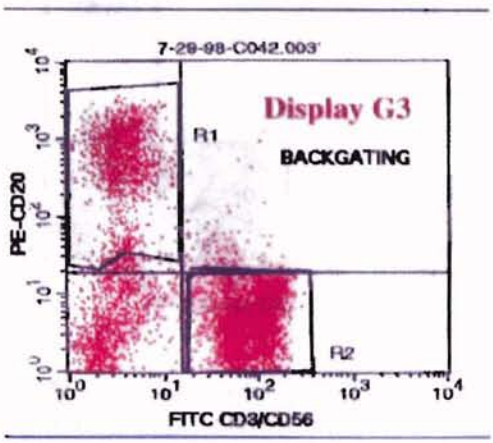

Figure 8f. Only events contained within an ungated light scatter plot to include events that represent the lymphocyte population.

Calculations for lymphocyte purity and recovery were as follows. Percent (%) Lymphocyte Recovery was calculated by dividing the number of events backgated from R3 (light scatter, ungated) and displayed in the R1 + R2 region of the fluorescent scatterplot (gated on R3), by the number of events confined to the R3 region drawn on the light scatter plot (gated on R1 + R2). % Lymphocyte Purity was calculated by dividing the number of events backgated from R3 (light scatter, ungated) and displayed in the R1 + R2 regions of the fluorescent scatterplot (gated on R3), by the number of events in the R3 region of the light scatterplot (ungated).

Gate optimization was performed by defining a new region, R4, on the same light scatterplot, and reformatting the graphs appropriately, so that R4 data replaced R3 data (Figure 8g and 8h).

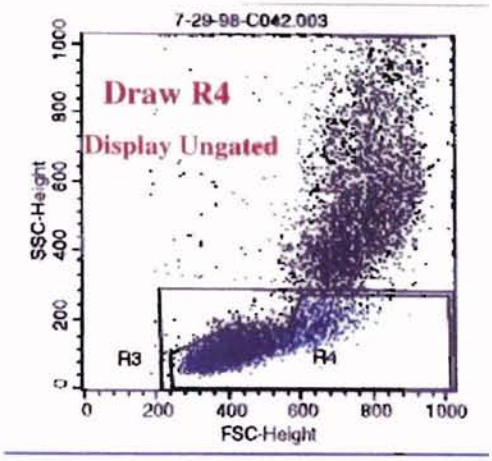

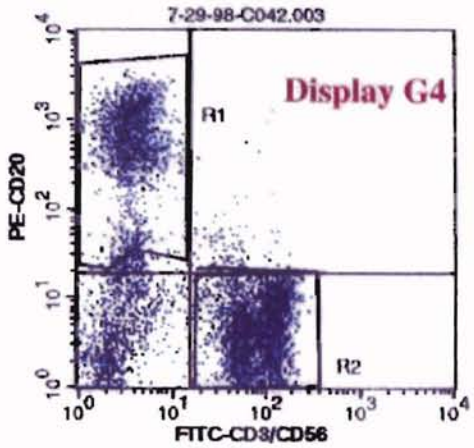

Figure 8g. Create and adjust R4 for optimization of purity and recovery. The R4 gate appears to exclude some lymphocyte events.

Figure 8h. Calculations for recovery and purity utilized data collected from fluorescent scatterplot gated to display only events contained within R4

Using the above calculations on the data collected, R4 was adjusted until the criteria for recovery (> 80%) and purity (>90%) was met, establishing the optimal lymphocyte gate. Appendix C summarizes hematologic values, quantification and percentages of events collected for these regions as described above, and results of the recovery and purity calculations. This data was collected on three samples run for each of 9 cynomolgus monkeys. With the exception of the 79.33% lymphocyte purity of the second sample run for monkey CO94, the NCCLS criteria was met in every case. Following its definition, all other samples from the panel were evaluated through this gate, and results were collected from each of four quadrants of a FL1/FL2 dot plot. These

results are provided in Appendixes D-G. Averages of these results are listed in Appendix B, which also lists results obtained from other previously reviewed literature.

EVALUATION OF GRAPHICAL DATA

For this study, in order to meet the minimal criteria of purity and recovery, definition of the R4 gate resulted in an area that becomes closely confluent with the uppermost portion of the lymphocyte cloud. The shape of the R4 gate was consistent throughout all monkeys and all samples assessed. The gate structure appears to exclude some events, presumed to be lymphocytes, in order to maintain quality control. In order to further evaluate what, if any, lymphoid events may have been excluded secondary to the defined gate perimeter; several regions were defined and assessed for one of the FITC-CD3/CD56 PE-CD20 samples (Figure 9a – 9d). Three regions were defined to include three distinct event clouds, on an ungated fluorescent dot-plot as depicted in figure 9a. These events are also depicted on an ungated light scatter plot (Figure 9b)

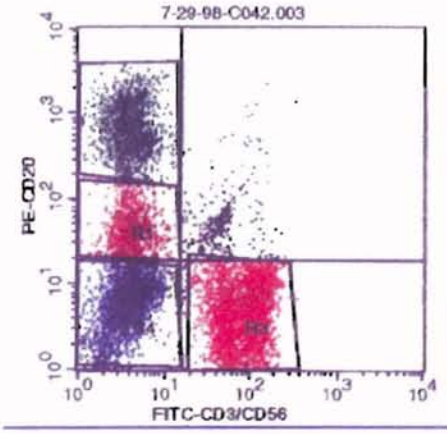

Figure 9a. User defined regions and colors are defined on fluorescent dot plot.

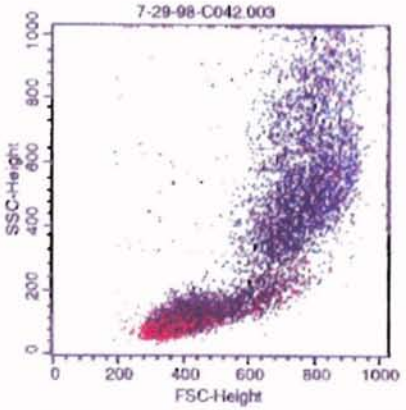

Figure 9b. All events of fluorescent plot are displayed on ungated light scatterplot.

These populations were assigned user-defined colors, and were further assessed on an ungated light scatter plot for evaluation of physical properties of cellular size and complexity. These defined regions isolated what appear to be four distinct cell populations. Based on fluorescent properties, these regions were presumed to represent cell populations as follows: R1 (orange)=B cells; R2 (green)=B cells; R3 (red)=All T and NK cells; U (blue)=unstained, negative population. The upper right quadrant also contains what is presumed to be nonlymphoid (undesired events). The ungated light scatterplot (Figure 9b) reveals a black (negative events) cell population at the uppermost aspect of the lymphocyte cloud. This suggests that many of these events are nonlymphoid, however, distinct resolution is not possible due to summation.

These cell populations were then assessed via a FL1/FSC scatter pot (Figure 9c). The combined use of fluorescence of FITC-CD3/CD56+ events and cellular size and complexity would allow isolation of small events displaying fluorescence, specifically the T and NK lymphocyte population. A cloud of FITC-CD3/CD56+ events (red cloud) with low FSC properties is revealed in figure 9c, which corresponds to the events contained with region R3 (Figure 9a). This cloud should represent all T and NK-cells, however, it is not completely delineated. There appears to be a small amount of continuous staining of green and black events, suggesting some B cell and nonlymphoid event fluorescent

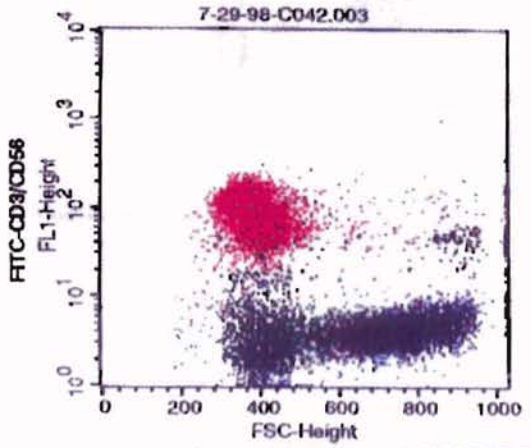

Figure 9c. FITC CD3/CD56 and FSC dot plot. The red cloud corresponds with T and NK lymphocyte populations.

overlap. Further, a small population of higher FSC black events also exhibits some FITC fluorescence, again suggesting some fluorescent overlap with the negative cell population. Additionally, another FL2/FSC graph was created to display PE-CD20+ fluorescence, which should represent all B lymphocytes (Figure 9d). Assessment of this plot reveals a green cloud that exhibits low FSC and high PE fluorescent intensity, corresponding to presumed B cells of R2. A smaller, apparently black cloud overlaps this population, again suggesting some fluorescent overlap with the presumed negative population. Previously described techniques limiting background fluorescence were performed prior to this analysis, which should have limited this overlap. Whether this overlap represents limitations in flow cytometric instrumentation, or operator errors in instrument optimization and control settings cannot be definitively determined. This overlap of apparent nonlymphoid events, however, appears to justify the final contours of the R4 lymphocyte gate.

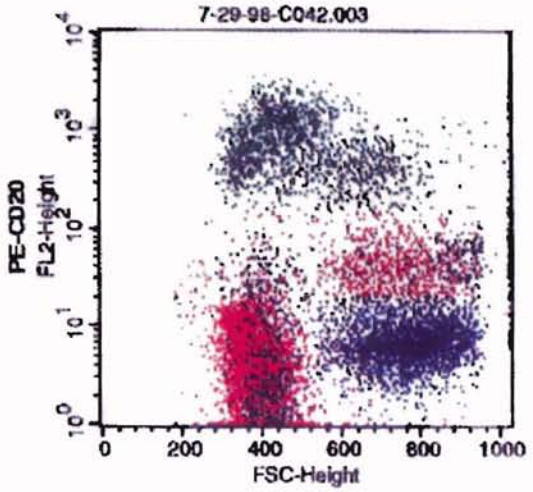

Figure 9d. FITC CD3/CD20 and FSC dot plot. The green cloud corresponds with B lymphocyte population

Also present on figure 9d is a distinct orange cloud of events, which displays a lower level of PE fluorescent intensity, and greater FSC properties than the B cell population. These cells may represent a larger, possibly reactive B-cell population, another distinct lymphoid population that also expresses CD20, or overlap with a nonlymphoid population, possibly monocytes, that exhibit weak PE fluorescence. Some

of this cloud was omitted by the confines of the original R1 gate (figure 9a). Whether these events should have been included in the final subtyping analysis remains undetermined.

Finally, the protocol used on the current study utilized the IgG isotype controls prior to establishing the lymphocyte gate. General guidelines and some previous research suggested this sequence of isotype control usage for lymphocyte subtyping. It is possible, however, that had the isotype controls been run following establishment of the lymphocyte gate, and confined within the R3 or R4 region (s), a larger amount of non-lymphoid events may have been excluded. More research is needed for clarification.

EVALUATION OF NUMERICAL DATA

Results from this study were comparable to reported findings of previously reviewed literature. Appendix B provides a summary of these results. No other research evaluated an anti-monkey CD3 as a pan-T cell marker, using instead an anti-human CD2 marker. This may reflect the unavailability of monkey-specific reagents at the time of this previous research. Rounded, averaged results for CD2 ranged from 56% - 76%, with a mode of 56%, and a mean of 65%. Averaged CD3 results for this study were 61% The range for CD4 was 28% - 53%, with a mode of 40% and a mean of 31.5%. Averaged CD4 results for this study were 29%. The range for CD8 was 25% - 48%, with a mode of 25% and a mean of 33%. Averaged CD4 results for this study were 33%. The range for CD20 was 12% - 25%, with a mean of 19%. Averaged CD20 results for this study were 22%. No CD56 results were provided in any of the research reviewed. Averaged results

of CD56 for this study were 4.80%. It appears that all results generated from this study were within the limits of previously reported research. Overall, the data from this research most closely resembles that reported by Verdier, et al., where averaged results for 312 male and female cynomolgus monkey CD2, CD4 and CD8 results were 56.5%, 29.5%, and 37%, respectively. The procedure used in this study was similar to that used by Verdier, with the exception that different clones were used, and no CD20 or CD56 results were provided. The actual lymphocyte gating protocol used by Verdier was not specifically described.

VII.

SUMMARY

Although only a limited number of studies specifically aimed at subtyping peripheral blood lymphocyte subpopulations in cynomolgus monkeys using flow cytometric immunophenotyping was available, results of this current study were well within the averaged values reported by this research. Discrepancies in actual numerical values among all studies may be attributed to variations in sample preparation, binding affinities of clones used, and/or gating techniques utilized. As previously stated, the general shape of the lymphocyte gate that resulted when lymphocyte recovery and purity was optimized during this project requires further investigation. What lymphocyte population, if any, and percentage thereof may have been excluded by the gate, remains undetermined. Assuming the general gate shape persists if this protocol is utilized, future studies may incorporate a more detailed evaluation of this gate phenomenon.

Although clone panels have been suggested (Verdier, et al), no specific gating technique has been described or submitted as part of any protocol. It is clear that a reproducible protocol, which includes lymphocyte gating optimization in accordance with NCCLS guidelines, is needed. This current study submits a complete protocol, which includes a panel of cross-reacting clones, and thoroughly describes a gating procedure, which, to the best of this author's knowledge, has not been previously described.

Additionally, further studies are needed to prove reproducibility of this proposed protocol, utilizing a larger sample population, and evaluating sequence of isotype control usage.

BIBLIOGRAPHY

Axberg, I., et al. (1991) "Characterization of T-Cell Subsets and T-Cell Receptor Subgroups in Pigtailed Macaques Using Two- and Three-Color Flow Cytometry."J.of Clin. Immuno. 11:4:193

Bleavins M. et al. (1993) "Flow Cytometric Characterization of Lymphocyte Subpopulations in the Cynomolgus Monkey." Vet Immuno and Immunopath. 37:1-13

Butel, J. Lednicky, J. (1999) "Cell and Molecular Biology of Simian Virus 40: Implication for human infection and Disease." Review. J. of the Natl. Cancer Inst. 91:2:117

Feichtinger, H. et al. (1990) "Malignant Lymphomas in Cynomolgus Monkeys Infected with Simian Immunodeficiency Virus." Am. J. of Pathology 137:6:1311

Feichtinger, H. et al. (1992) " A Monkey Model for Epstein-Barr Virus-associated Lymphomagenesis in Human Acquired Immunodeficiency Syndrome." J. Exp. Med July 176: 281-286

Ganguly NK, et al. (1977) "T and B cell Populations in Peripheral Whole Blood of Rhesus Monkeys." Int. Arch Allergy Applied Imm. 53:290-292

Gratama, J.W., et al (1998) "Flow Cytometric Quantification of Immunofluorescent Intensity: Problems and Perspectives." Cytometry 33:2:166

Jacobsen, C.N. et al. (1993) "Reactivities of 20 Anti-Human Monoclonal Antibodies with Leukocytes from 10 Different Animal Species." Vet. Immuno. And Immunopath. 39:461-466

Kesterson, J.W. (1982) Drug Safety Evaluation: Animal Toxicology Studies and their Interpretations. Drug Information Journal January/June p. 81

Kneitz, C., et al. (1993) "Early Phenotypic and Functional Alterations in Lymphocytes from Simian Immunodeficiency Virus Infected Macaques." Vet. Immuno and Immunopath. 36:239-255

Li, Su-Ling, et al. (1993) "Immunohistochemical Distribution of Leucocyte Antigens in Lymphoid Tissues of Cynomolgus Monkeys (*Macaca fascicularis*)." J. of Med. Primatology 22:285-293

Loken, M.R., et al. (1990) "Establishing Optimal Lymphocyte Gates for Immunophenotyping by Flow Cytometry." Cytometry 11:453-459

Maggiorella, M.T., et al.(1998) "Detection of Infectious Simian Immunodeficiency Virus in B- and T-Cell Lymphomas of Experimentally Infected Macaques." Blood 91:9:3103

Picker L.J. (1998) "Identification of Functional Subsets by Flow Cytometry: Intracellular Detection of Cytokine Expression." Cytometry 34:5:207

Putkonen, P. et al. (1992) "Clinical Features and Predictive Markers of Disease Progression in Cynomolgus Monkeys Experimentally Infected with Simian Immunodeficiency Virus." AIDS 6:3:257

Reimann, K.A., et al. (1994) "Use of Human Leukocyte-Specific Antibodies for Clinically Immunophenotyping Lymphocytes of Rhesus Monkeys." Cytometry 17:102-108

Rezikyan, s. et al. (1995) "B-Cell Lymphomagenesis in SIV-Immunosuppressed Cynomolgus Monkeys." Int. J. Cancer 61:574-579

Sopper, S., et al. (1997) "Lymphocyte Subsets and Expression of Differentiation Markers in Blood and Lymphoid Organs of Rhesus Monkeys." Cytometry 29:351-162

Verdier, F et al. (1992) "Characterization of Lymphocyte Subtypes in Cynomolgus Monkeys Using Flow Cytometry. Influence of Methylprenisolone." Tox Methods. 1:263-272

Yasuko, K., et al. (1989) "Phenotypic Characterization of Cynomolgus Monkey Natural Killer Cells." Cellular Immun. 122:524-533

REFERENCES

1. Baronelli, S. et al. (1997) "Longitudinal Characterization of CD4, CD8 T cell subsets and of Haematological Parameters in Healthy Newborn Cynomolgus Monkeys." Vet Immuno and Immunopath. 59:141-150

2. Bleavins M. et al. (1993) "Flow Cytometric Characterization of Lymphocyte Subpopulations in the Cynomolgus Monkey." Vet Immuno and Immunopath. 37:1-13

3. FACSCalibur System User's Guide-Becton-Dickenson Immunocytochemistry Systems.

4. Gosset, K, et al. (1999) "Flow Cytometry in the Preclinical Development of Biopharmaceuticals." Tox. Path. 27:1:32

5. Kantor, Roederer (1996) "FACS Analysis of Leukocytes" Handbook of Experimental Immunology 5th Edition. Herzenberg, Weir, Blackwell

6. Letvin, N.L., et al. (1983) "T Lymphocyte Surface Antigens in Primates." Eur. J. Immun. 13:345-347

7. Mandy F.F., et al (1997) "Evaluation of Lymphocyte Immunophenotypes as Influenced by the HIV/AIDS Pandemic: A Short History of the Development of Gating Strategies for CD4+ T-Cell Enumeration." Cytometry 30:4:157

8. Quadrant Correction/Percent Lymphocyte Conversion. Cytometry Source Book – Becton-Dickenson Immunocytometry Systems 1998

9. Reichert, T., et al. (1991) "Lymphocyte Subset Reference Ranges in Adult Caucasians." Clin. Immun. and Immunopath. 60:190-208

10. Sagara N, et al. (1990) "Characterization of Lymphocyte Subpopulations in the Blood of Cynomolgus Monkeys using Flow Cytometry." Jour. Of Appl. Tox. 10:3:211

11. Tatsumi, et al. (1982) "Identification of Cytotoxic T Lymphocytes by Alpha-Naphthyl Acetate Esterase Staining and Spontaneous Erythrocyte Rosette Formation." Am. J. of Prim. 3:99-110

12. Terrell, TG, et al. (1977) "Immunologic Surface Markers on Non-Human Primate Lymphocytes." Am. J. of Vet. Res. 38:503-507

13. Tryphonas, H., et al. (1996) "Cell Surface marker Evaluation of Infant *Macaca* Monkey Leukocytes in Peripheral Whole Blood using Simultaneous Dual-Color Immunophenotypic Analysis." J. of Med. Primatology 25:89-105

14. Verdier F., et al (1995) "Detection of Lymphocyte Subsets and Cytokine Levels in Cynomolgus Monkeys" Toxicology 105:1:81

15. Verdier F., et al. (1992) "Characterization of Lymphocyte Subtypes in Cynomolgus Monkeys Using Flow Cytometry. Influence of Methylprenisolone." Tox Methods. 1:263-272

16. Villas, B.H. (1998) "Flow Cytometry: An Overview." Cell Vis 5:1:56

APPENDIX A.

Commercial monoclonal antibodies tested for cross reactivity.

Source	Antibody	Clone	Label	Isotype	Host	Amount (total per test)	Reactivity *	Catalog #
Serotec	CD3 (anti-monkey)	FN18	FITC	IgG1	mouse	5 ml/50 ul	Positive	MCA1483F **
	CD8	LT8	PE	IgG1	mouse	1 ml/10 ul	Not listed	MCA1226P
	CD8	YTC 182.20	FITC	IgG1	rat	1 ml/10 ul	Not listed	MCA351F
	CD16	LNK16	PE	IgG2b	mouse	1 ml/10 ul	Not listed	MCA1193P
	CD20	B-H20	PE	IgG1	mouse	1 ml/10 ul	Not listed	MCA953P **
	CD56	B-A19	PE	IgG1	mouse	1 ml/10 ul	Not listed	MCA670P
Biosource	CD3 (anti-monkey)	FN18	FITC	IgG1	mouse	1 ml/10 ul	Positive	APS0308
	CD4	EDU-2	PE	IgG2a	mouse	1 ml/10 ul	Not listed	AHS0417
	CD16	B-E16	PE	IgG1	mouse	1 ml/10 ul	Positive	AHS1607
				I				
DAKO	CD4	MT310	PE	IgG1	mouse	1 ml/10 ul	Positive	R0805 **
	CD8	DK25	PE	IgG1	mouse	1 ml/10 ul	Positive	R0806 **
	CD20	B-Ly1	PE	IgG1	mouse	1 ml/10 ul	Positive	R7013
	CD56	MOC1	PE	IgG1	mouse	1 ml/10 ul	Positive	R7127
Coulter	CD8	B911	PE	IgG1	mouse	2 ml/20 ul	Positive	IM0452
	CD16	3G8	PE	IgG1	mouse	2 ml/20 ul	Positive	IM1238
	CD20	B9E9	PE	IgG2a	mouse	2 ml/20 ul	Not listed	IM1451
Becton-Dickinson	CD4	SK3	PE	IgG1	mouse	2 ml/20 ul	Positive	347327
	CD14	MOP9	PE	IgG2b	mouse	2 ml/20 ul	Not listed	347497
	CD16	NKP15	FITC	IgG1	mouse	2 ml/20 ul	Not listed	347627
	CD45	L243	FITC	IgG2a	mouse	2 ml/20 ul	Not listed	347427
	CD56	MY31	PE	IgG1	mouse	2 ml/20 ul	Negative	347747 **
	CD56	Leu-19	PE	IgG1	mouse	2 ml/20 ul	Not listed	347697
Pharmingen	CD14	M5E2	PE	IgG2a	mouse	2 ml/20 ul	Not listed	30545X
	CD20	2H7	PE	Ig2b1	mouse	2 ml/20 ul	Not listed	33265X
	CD21	B-Ly4	PE	IgG1	mouse	2 ml/20 ul	Not listed	30695X
Serotec (isotype controls)	IgG1		FITC		mouse	100T		MCA928F **
	IgG1		PE		mouse	100T		MCA928P **
	IgG2a		PE		mouse	100T		MCA929P
	IgG2b		FITC		rat	100T		MCA1125F

*Cross-reactivity of human clone with cynomolgus monkeys if known.
**Final panel of antibodies and isotype controls selected for this research

APPENDIX B.

Summary of results from literature and the current study.

Author	# of subjects in sample	Antigens Targeted	Antibody clones	Label	Results (%)		
					Male	Pooled	Female
Levtin (1983)	7	CD2	T12	FITC		56 +/- 9	
		CD4	T4	FITC		33 +/- 16	
		CD8	T8	FITC		25 +/- 11	
Sagara (1990)	30f	T cells	T11	FITC		72.1 +/- 2.4	
		B cells	Anti-monkey	FITC		24.6 +/- 2.4	
Bleavins (1993)	69m	CD4	Anti-leu 3a	PE	28		30
	77f	CD8	Anti-leu 2a	PE	56		54
		CD20	Anti-leu 16	PE		12	
Verdier (1995)	153m	CD2	Anti-leu 16	FITC	56 +/- 18		57 +/- 17
	159f	CD4	OKT4	FITC	30 +/- 11		29 +/- 11
		CD8	Anti-leu 2a	PE	37 +/- 14		37 +/- 14
		CD20	Anti-leu 16	FITC		no results listed	
Tryphonas (1996)	6m	CD2	Ortho	FITC	*75.57 +/- 4.85		77.5+/- 4.85
	6f	CD2	BD	FITC			
		CD4	Ortho	FITC	*40.07 +/- 8.18		53.3+/- 3.72
		CD4	BD	PE			
		CD8	Ortho	FITC	*48.57 +/- 9.06		38.61+/- 3.34
		CD8	BD	PE			
		CD16	Ortho	FITC		no results listed	
		CD16	BD	PE			
		CD20	BD	PE	23.14 +/- 3.21		19.96+/- 3.60
					*Results were pooled when multiple clones for individual antigens were used.		
Baronecelli (1997)	17m	CD4	DAKO MT310	PE		40.5	
	20f	CD8	DAKO DK25	FITC		25.5	
Decker (1998)	6m	CD3	Biosource FN18	FITC		60.79**	
	3f	CD4	DAKO MT310	PE		28.75	
		CD8	DAKO DK25	PE		33.50	
		CD20	Serotec B H2O	PE		22.40	
		CD56	BD MY31	PE		4.80	

m=male, f=female

** Results were averaged from CD3/CD20 and CD3/CD56 samples only.

APPENDIX C

Hematologic values and results of calculations for lymphocyte recovery

MONKEY	TWBCC	LVM	%LVM	SC R4 NO GATE D3/20/56		SC R3 NO GAT E CD3/20/56		FL R1 + R2 CD3/20/56				% PURITY FL G3(R1+R2) /G3(R3)	% RECOVER FLG3(R1+2 FLG4(R1+R
								G=R4 EVENT (R1+R2)	G=R4 %GT	G=R3 EVENT (R1+R2)	G=R3 %GT		
				EVE	% GAT	EVE	% GAT						
C053 7/28	13.7	8.39	61.2	6393	63.93	5104	51.04	4525	70.78	4094	80.21	80.21	90.4
C053 7/29 R1				6663	66.63	5493	54.93	5001	75.05	4511	82.13	82.13	90.2
C053 7/29 R2				6893	68.93	5099	59.99	5185	75.23	4829	80.50	80.50	93.1
C057 7/28	16.2	11.7	72.3	7784	77.84	69.55	69.55	6374	81.88	6088	87.53	87.53	95.5
C057 7/29 R1				7798	77.98	7145	71.45	6351	81.44	6106	85.45	85.45	96.1
C057 7/29 R2				7498	74.98	6597	65.97	6101	81.37	5627	85.3	85.3	92.2
C061 7/28	12.5	8.54	68.3	7506	75.06	6190	61.90	6030	80.34	5520	89.18	89.18	91.5
C061 7/29 R1				7488	74.88	6481	64.81	5606	74.84	5200	80.23	80.23	92.8
C061 7/29 R2				7494	74.94	6525	65.25	5657	75.49	5317	81.49	81.49	94.0
C042 7/28	17.2	11.0	64.0	6214	62.14	5400	54.0	5290	85.13	4822	89.3	89.3	91.2
C042 7/29 R1				6122	61.22	5587	55.87	4915	80.28	4655	83.32	83.32	94.7
C042 7/29 R2				6331	63.31	5889	58.89	5166	81.60	4981	84.58	84.58	96.4
C074 7/28	13.7	4.87	53.0	5467	54.67	4229	42.29	3969	72.60	3660	86.54	86.54	92.2
C074 7/29 R1				5655	56.55	4606	46.06	3971	70.22	3660	79.46	79.46	92.2
C074 7/29 R2				5684	56.84	4476	44.76	3973	69.90	3602	80.47	80.47	90.7
C094 7/28	11.1	5.22	47.1	4948	49.48	4296	42.96	3706	74.9	3504	81.56	81.56	94.5
C094 7/29 R1				4672	46.72	3580	35.80	3344	71.57	2840	79.33	79.33	84.92
C094 7/29 R2				4861	48.61	4025	40.25	3582	73.69	3232	80.3	80.3	90.2
A405 7/28	12.1	2.43	20.0	2094	20.94	1835	18.35	1847	88.20	1674	91.23	91.23	90.6
A405 7/29 R1				2161	21.61	1882	18.82	1779	82.33	1616	85.86		90.8
A405 7/29 R2				2151	21.51	1897	18.97	1817	84.65	1650	86.98		90.8
A453 7/28	6.08	2.37	39.0	3948	39.48	3606	36.06	3681	93.23	3478	96.45	96.45	94.5
A453 7/29 R1				3290	32.90	2779	27.79	2602	79.06	2351	84.60	84.60	90.4
A453 7/29 R2				3239	32.39	2928	29.28	2645	81.66	2494	85.18	85.18	94.3
B065 7/28	11.2	3.42	30.5	3101	31.01	2760	27.60	2659	85.75	2459	89.09	89.09	92.5
B065 7/29 R1				4070	40.70	3738	37.38	3751	92.16	3515	94.0	94.0	94.1
B065 7/29 R2				4210	42.10	3831	38.31	3826	90.88	3608	94.2	94.2	
1RC042 7//29	18.5	12.5	67.9	5453	54.53	4831	48.31	4486	82.27	4141	85.72	85.72	92.3
2RC042 7/29				5533	55.33	4866	48.66	4328	78.22	3923	80.62	80.62	90.6

APPENDIX D

Summary of Data for CD3/CD4. All final runs and monkeys tested.

CD3/CD4 MONKEY	G3 TOTAL EVENTS	UL CD3-CD4+		UR CD3+/CD4+		LL UNSTAINED		LR CD3+	
		EVNT	%	EVNT	%	EVNT	%	EVNT	%
C053 7/28	4717	62	1.31	1097	23.26	2228	47.23	1330	28.20
C053 7/29 R1	4730	367	7.76	1151	24.33	2038	43.09	1174	24.82
C053 7/29 R2	5596	631	11.28	1352	24.16	2322	41.49	1291	23.07
C057 7/28	6668	111	1.62	2309	33.62	2469	35.95	1979	28.81
C057 7/29 R1	7115	98	1.38	2240	31.48	2888	40.59	1889	26.55
C057 7/29 R2	6567	48	0.73	2206	33.59	2441	37.17	1872	28.51
C061 7/28	6018	57	0.95	1740	28.91	2196	36.49	2025	33.65
C061 7/29 R1	6277	30	0.48	1742	27.75	2493	39.72	2012	32.05
C061 7/29 R2	6270	23	0.37	1678	26.76	2390	38.12	2179	34.75
C042 7/28	5731	33	0.58	2143	37.39	1866	32.56	1689	29.47
C042 7/29 R1	5720	25	0.44	1980	34.62	2012	35.17	1703	29.77
C042 7/29 R2	6075	40	0.66	2150	35.39	2160	35.56	1725	28.40
C074 7/28	4321	30	0.69	1279	29.60	1965	45.48	1047	24.23
C074 7/29 R1	4518	21	0.46	1227	27.16	2250	49.80	1020	22.58
C074 7/29 R2	4319	25	0.58	1220	28.25	2026	46.91	1048	24.26
C094 7/28	4193	38	0.91	1713	40.85	1488	35.49	954	22.75
C094 7/29 R1	3646	6	0.16	1505	41.28	1236	33.90	899	24.66
C094 7/29 R2	4158	17	0.41	1657	39.85	1565	37.64	919	22.10
A405 7/28	2096	24	1.15	756	36.07	639	30.49	677	32.20
A405 7/29 R1	2280	23	1.01	736	32.28	801	35.13	720	31.58
A405 7/29 R2	2158	27	1.25	745	34.52	686	31.79	700	32.44
A453 7/28	3428	27	0.79	1349	39.35	984	28.70	1068	31.16
A453 7/29 R1	2826	11	0.39	702	24.84	799	28.27	1314	46.50
A453 7/29 R2	2800	15	0.54	716	25.57	821	29.32	1248	44.57
B065 7/28	2715	20	0.74	767	28.25	778	28.66	1150	42.36
B065 7/29 R1	3870	45	1.16	1363	35.22	1294	33.44	1168	30.18
B065 7/29 R2	3726	37	0.99	1384	37.14	1142	30.65	1163	31.21
1RC042 7/29	4614	56	1.21	1232	26.70	1869	40.51	1457	31.58
2RC042 7/29	4449	64	1.44	1174	26.39	1921	43.18	1290	29.00

APPENDIX E

Summary of Data for CD3/CD8. All final runs and monkeys tested.

CD3/CD8 MONKEY	G3 TOTAL EVENTS	UL CD3-CD8+		UR CD3+/CD8+		LL UNSTAINED		LR CD3+	
		EVNT	%	EVNT	%	EVNT	%	EVNT	%
C053 7/28	4463	1274	28.55	1361	30.50	1034	23.17	1034	17.79
C053 7/29 R1	4648	1496	32.19	1422	30.59	1013	21.79	717	15.43
C053 7/29 R2	5191	1687	32.50	1504	28.97	1336	25.74	664	12.79
CO57 7/28	6927	1239	17.89	2389	34.49	1351	19.50	1948	28.12
C057 7/29 R1	6972	1370	19.65	2295	32.92	1400	20.08	1907	27.35
C057 7/29 R2	6564	1317	20.06	2342	35.68	981	14.95	1924	29.31
C061 7/28	6210	1246	20.06	2411	38.82	1011	16.28	1542	24.83
C061 7/29 R1	6567	1418	21.59	2414	36.76	1106	16.84	1629	24.81
C061 7/29 R2	6609	1422	21.52	2361	35.72	1162	17.58	1664	25.18
C042 7/28	5458	580	10.63	1809	33.14	1146	21.00	1923	35.23
C042 7/29 R1	5607	650	11.59	1690	30.14	1323	23.6	1944	34.67
C042 7/29 R2	5830	591	10.14	1730	29.67	1529	26.23	1980	33.96
C074 7/28	4481	574	12.81	1132	25.26	1545	34.48	1230	27.45
C074 7/29 R1	4767	462	9.69	2341	49.11	367	7.70	1597	33.50
	4767	(787)	(16.51)	(1049)	(22.01)			(1323)	(27.75)
C074 7/29 R2	4541	396	8.72	2276	50.12	341	7.51	1528	33.65
	4541	(701)	(15.44)	(1020)	(22.46)			(1292)	(28.45)
C094 7/28	4218	835	19.80	892	21.15	775	18.37	1716	40.68
C094 7/29 R1	3598	647	17.98	774	21.51	655	18.20	1522	42.30
C094 7/29 R2	4067	802	19.72	942	23.16	755	18.56	1568	38.55
A405 7/28	1958	119	6.08	754	38.51	442	22.57	643	32.84
A405 7/29 R1	2435	119	4.89	722	29.65	949	38.97	645	26.49
A405 7/29 R2	2344	121	5.16	781	33.32	764	32.59	678	28.92
A453 7/28	3332	247	7.41	958	28.78	759	22.78	1368	41.06
A453 7/29 R1	2681	364	13.58	1235	46.06	433	16.15	649	24.21
A453 7/29 R2	2733	265	9.70	1217	44.53	587	21.48	664	24.30
B065 7/28	2661	308	11.57	1134	42.62	509	19.13	710	26.68
B065 7/29 R1	4025	248	6.16	1027	25.52	1385	34.41	1365	33.91
B065 7/29 R2	3727	272	7.30	1059	28.41	976	26.19	1420	38.10
1RC042 7/29	4622	672	14.54	1706	36.91	1239	26.81	1005	21.74
2RC042 7/29	4504	738	16.39	1512	33.57	1323	29.37	931	20.67

APPENDIX F

Summary of Data for CD3/CD20. All final runs and monkeys tested.

CD3/CD20 MONKEY	G3 TOTAL EVENTS	UL CD3-CD20+		UR CD3+/CD20+		LL UNSTAINED		LR CD3+	
		EVNT	%	EVNT	%	EVNT	%	EVNT	%
C053 7/28	4568	1335	29.23	133	2.91	1081	23.66	2019	44.20
C053 7/29 R1	4865	1419	29.17	353	7.26	1258	25.86	1835	37.72
C053 7/29 R2	5218	1622	31.08	332	6.36	1379	26.43	1885	36.12
CO57 7/28	6894	1863	27.02	210	3.05	769	11.15	4052	58.78
C057 7/29 R1	7133	1673	23.45	255	3.57	1151	16.14	4054	56.83
C057 7/29 R2	6517	1425	21.87	232	3.56	984	15.10	3876	59.48
C061 7/28	6096	1409	23.11	183	3.00	802	13.16	3702	60.73
C061 7/29 R1	6350	1231	19.39	151	2.38	1250	19.69	3718	58.55
C061 7/29 R2	6551	1368	20.88	170	2.60	1242	18.96	3771	57.56
C042 7/28	5710	1298	22.73	244	4.27	644	11.28	3524	61.72
C042 7/29 R1	5505	1192	21.65	220	4.00	838	15.22	3255	59.13
C042 7/29 R2	5685	1358	23.89	196	3.45	705	12.40	3426	60.29
C074 7/28	4312	1442	33.44	140	3.25	630	14.61	2100	48.70
C074 7/29 R1	4559	1323	29.02	127	2.79	1051	23.05	2058	45.14
C074 7/29 R2	4200	1282	30.52	123	2.93	676	16.10	2119	50.45
C094 7/28	4446	1020	22.94	96	2.16	672	15.11	2658	59.78
C094 7/29 R1	3807	782	20.54	27	0.71	637	16.73	2361	62.02
C094 7/29 R2	4121	876	21.26	43	1.04	700	16.99	2502	60.71
A405 7/28	1967	412	20.95	75	3.81	158	8.03	1322	67.21
A405 7/29 R1	2544	327	12.85	9	0.35	696	27.36	1512	59.43
A405 7/29 R2	2428	350	14.42	3	0.12	551	22.69	1524	62.77
A453 7/28	3423	844	24.66	119	3.48	189	5.52	2271	66.35
A453 7/29 R1	2808	368	13.11	27	0.96	505	17.98	1908	67.95
A453 7/29 R2	2849	377	13.23	25	0.88	487	17.09	1960	68.80
B065 7/28	2855	456	15.97	89	3.12	388	13.59	1922	67.32
B065 7/29 R1	4496	842	18.73	30	0.67	1185	29.36	2439	54.25
B065 7/29 R2	3882	805	20.74	19	0.49	499	12.85	2559	65.92
1RC042 7/29	4501	1229	27.31	419	9.31	650	14.44	2203	48.94
2RC042 7/29	4346	1286	29.59	408	9.39	662	15.23	1990	45.79

APPENDIX G

Summary of Data for CD3/CD56. All final runs and monkeys tested.

CD3/CD56 MONKEY	G3 TOTAL EVENTS	UL CD3-CD56+		UR CD3+/CD56+		LL UNSTAINED		LR CD3+	
		EVNT	%	EVNT	%	EVNT	%	EVNT	%
C053 7/28	4595	240	5.22	210	4.57	2060	44.83	2085	45.83
C053 7/29 R1	4835	570	11.79	689	14.25	1831	37.87	1745	36.09
C053 7/29 R2	5563	794	14.27	874	15.71	2023	36.37	1872	33.65
	5563	()	()	()	()	()	()	()	()
CO57 7/28	6920	1	0.01	160	2.31	2376	34.34	4383	63.34
C057 7/29 R1	7193	25	0.35	933	12.97	2449	34.05	3786	52.63
								(4432)	(61.62)
C057 7/29 R2	6707	15	0.22	845	12.60	2124	31.67	3723	55.51
								(4341)	(64.72)
C061 7/28	6180	421	6.81	267	4.32	1805	29.21	3687	59.66
C061 7/29 R1	6588	272	4.13	83	1.26	2331	35.38	3902	59.23
C061 7/29 R2	6630	339	5.11	89	1.34	2214	33.39	3988	60.15
C042 7/28	5593	279	5.02	282	5.07	1557	27.99	3445	61.93
C042 7/29 R1	5482	199	3.63	89	1.62	1838	33.53	3356	61.22
C042 7/29 R2	5617	304	5.41	111	1.98	1800	32.05	33402	60.57
C074 7/28	4231	118	2.79	127	3.00	1820	43.02	2166	51.19
C074 7/29 R1	4512	130	2.88	167	3.70	2186	48.45	2029	44.97
C074 7/29 R2	4182	108	2.58	162	3.87	1876	44.86	2036	48.68
C094 7/28	4361	94	2.16	127	2.91	1447	33.18	2693	61.75
C094 7/29 R1	3464	30	0.87	168	4.85	1043	30.11	2223	64.17
C094 7/29 R2	4121	876	21.26	43	1.04	700	16.99	2502	60.71
A405 7/28	1937	178	9.19	113	5.83	363	18.74	1283	66.24
A405 7/29 R1	2033	193	9.49	37	1.82	538	26.46	1265	62.22
A405 7/29 R2	2048	202	9.86	42	2.05	460	22.46	1344	65.62
A453 7/28	3299	180	5.46	81	2.46	646	19.58	2392	72.51
A453 7/29 R1	2661	75	2.82	26	0.98	707	26.57	1853	69.64
A453 7/29 R2	2865	147	5.13	23	0.80	770	26.88	1925	67.19
B065 7/28	2739	128	4.67	114	4.16	665	24.28	1832	66.89
B065 7/29 R1	4223	185	4.38	190	4.50	1276	30.22	2572	60.90
B065 7/29 R2	3993	215	5.38	178	4.46	1103	27.62	2497	62.53
1RC042 7/29	4337	378	8.72	348	8.02	1434	33.06	2177	50.20
2RC042 7/29	4298	451	10.49	331	7.70	1594	37.09	1922	44.72

VITA

Lilli Decker

Candidate for the Degree of

Master of Science

Thesis: IMMUNOPHENOTYPING AND TWO-COLOR FLOW CYTOMETRY: STRATEGIES OF OPERATION AND LYMPHOCYTE GATING FOR SUBTYPING LYMPHOCYTE POPULATIONS IN PERIPHERAL WHOLE BLOOD OF CYNOMOLGUS MONKEYS.

Major Field: Veterinary Biomedical Sciences

Biographical:

Education: Graduated from Smithtown High School East, St. James, NY in May 1980; received Bachelor of Science in Natural Science and Mathematics and triple certification for Secondary Education in mathematics, biology, and chemistry from Dowling College, Oakdale, NY in May 1992 and May 1993, respectively; received degree of Doctor of Veterinary Medicine from Oklahoma State University, College of Veterinary Medicine in May 1997. Completed the requirements for the Master of Science degree in Veterinary Biomedical Sciences at Oklahoma State University in May, 2000.

Experience: Professional tutor for Academic Services at Dowling College; employed as veterinary technician at Animal Emergency Hospital in Commack, NY; employed as emergency laboratory technician at Oklahoma State University; Boren Veterinary Medicine Teaching Hospital; employed by Oklahoma State University, Department of Anatomy, Physiology and Pharmacology as teaching assistant in endocrinology; employed by Oklahoma State University, Department of Anatomy, Physiology and Pharmacology as a graduate research assistant and a clinical pathology resident; presently employed by Antech Diagnostic Laboratories in Farmingdale, NY while completing clinical pathology residency requirements.

Professional Memberships: American Society of Veterinary Clinical Pathologists; American Veterinary Medicine Association.